Report NOV. 2003 on:

Numerical model estimates of tidal conversion

Global estimates of tidal conversion

Emanuele Di Lorenzo

Numerical model estimates of tidal conversion

A first step towards incorporating parameterizations of internal tides generation into climate models is to take a state of the art primitive equation ocean numerical model and test its ability to capture the dynamics of internal tides generation.

For this purpose numerical estimates of the tidal conversion rate are performed with the Regional Ocean Modeling System (ROMS, publicly available on the web http://marine.rutgers.edu/po/index.php?model=roms) and then compared with the predictions from theory in both the WTA and super-critical limits.

The ROMS model solves the ocean primitive equation on a curvilinear horizontal grid and on a generalized s-coordinate system in the vertical. This modeling system has been used to successfully model a wide variety of realistic coastal flows (Di Lorenzo, 2003: Di Lorenzo et al., 2003: Haidvogel et al., 1991: Hermann and Stabeno, 1996: Marchesiello et al., 2003) and basin scale circulations (Haidvogel et al., 2000). The model uses higher order numerics (Shchepetkin and McWilliams, 1998: 2003). The code is highly modular and the user can select the use of different types of advection schemes, vertical mixing scheme, tides, biology, floats, etc. Recently Moore et al. (2003) have also implemented the tangent and adjoint models for ROMS, a set of tools that can be used for dynamical stability analysis as well as for data assimilation problems. All these features make ROMS a good candidate for the next generation climate model and therefore was chosen for our numerical experiments.

To estimate the conversion rates in the numerical model we configure a rectangular basin of dimensions 900 x 9 (x,y) km. The grid resolution is 1.5 km in the horizontal. In the vertical 40 levels are equally spaced to cover the total depth of the model's ocean (H = 2000 meters). At the center of the domain we position a gaussian ridge of height h_{max} and width 5 km. The along ridge direction is along the y-axis (9 km). The model has four open boundaries. Periodic boundary conditions are applied in the y-direction and radiation conditions are applied in the x-direction. The model does not use any explicit horizontal dissipation except close the x boundaries. In the vertical we use a viscosity and diffusivity coefficient of 10^{-3} m^2/s and no explicit mix layer scheme. At the bottom a free-slip condition is used with no bottom drag. We solve the linearized problem. The non-linear case experiments were also performed for the WTA limit and no differences were noted in the conversion rate. Full exploration of the super-critical regime with the non-linear dynamics is still pending. The model is forced with the M2 barotropic tide through the open boundaries in the x-direction. The tide is introduced by specifying the M2 free-surface elevation and barotropic velocity at the open boundaries in x.

We perform a set of model conversion estimates varying the height of the gaussian ridge and the stratification (N). The results (Fig. 1) show that the model conversion estimates agree with the one from theory in both the WTA and super-critical regimes. We present two different estimates for the model conversion: (1) the conversion over the ridge from the barotropic to baroclinic tides and (2) the radiated wave energy flux through the eastern and western walls located away from the ridge. We find that the radiated flux of wave energy is generally less than the conversion over the ridge. This indicates that some of the baroclinic energy generated over the ridge is dissipated as the waves propagate in the medium. The fraction of energy dissipated increases as we progress towards more super-critical regime. One possible explanation comes from the theory results that predict very steep unstable slopes at the edges of the generated beams. The model (at this resolution and with this vertical viscosity/diffusivity) captures the early phase of these instabilities close to the gaussian ridge (Fig.2), but as the internal tide propagates away from the ridge these instabilities are dissipated and therefore some of the baroclinic energy is lost. However the fraction of dissipated energy is small compared to the total.

We will continue to investigate the model sensitivity to a decrease in the vertical viscosity/diffusivity and an increase in the horizontal resolution. We will also explore a wider range of model dynamics by introducing non-linear effects, bottom drag and no-slip boundary conditions.

Global estimates of tidal conversion

A second step toward designing parameterizations of the internal tides for climate models is to use the available theoretical model in combination with the topographic measurements to estimate the conversion rate. For this purpose we have developed a set of numerical tools to aid the calculation of global conversion rates. These tools relay on a world ocean topographic dataset (currently we are using Sandwell and Smith TOPEX data) and tidal ellipses estimates (from the TPXO 6.0 product). Figure 3 shows an example of extracting topography and tidal ellipses for a particular portion of ocean. The topography is then converted into power spectra's that are used for the calculation of conversion rates. We have not yet done a global estimate. We intend to do that after we complete the validation of these numerical calculations against conversions obtained from analytical topographic cases and model simulations with more realistic topography.

References

Di Lorenzo, E., 2003: Seasonal dynamics of the surface circulation in the Southern California Current System. *Deep Sea Research Part II: Topical Studies in Oceanography*, **50,** 2371-2388.

Di Lorenzo, E., M. G. G. Foreman, and W. R. Crawford, 2003: Modeling the generation of Haida eddies. *Deep-Sea Research II***,** submitted.

Haidvogel, D. B., A. Beckmann, and K. S. Hedstrom, 1991: Dynamic Simulations of Filament Formation and Evolution in the Coastal Transition Zone. *Journal of Geophysical Research-Oceans*, **96,** 15017-15040.

Haidvogel, D. B., H. G. Arango, K. Hedstrom, A. Beckmann, P. Malanotte-Rizzoli, and A. F. Shchepetkin, 2000: Model evaluation experiments in the North Atlantic Basin: simulations in nonlinear terrain-following coordinates. *Dynamics of Atmospheres and Oceans*, **32,** 239-281.

Hermann, A. J. and P. J. Stabeno, 1996: An eddy-resolving model of circulation on the western Gulf of Alaska shelf .1. Model development and sensitivity analyses. *Journal of Geophysical Research-Oceans*, **101,** 1129-1149.

Marchesiello, P., J. C. McWilliams, and A. Shchepetkin, 2003: Equilibrium structure and dynamics of the California Current System. *Journal of Physical Oceanography*, **33,** 753-783.

Moore, A., H. Arango, B. D. Cornuelle, E. Di Lorenzo, A. J. Miller, and D. J. Neilson, 2003: The ROMS Tangent Linear and Adjoint Models: A Comprehensive Ocean Prediction System**,** manuscript in prep.

Shchepetkin, A. F. and J. C. McWilliams, 1998: Quasi-monotone advection schemes based on explicit locally adaptive dissipation. *Monthly Weather Review*, **126,** 1541-1580.

——, 2003: A method for computing horizontal pressure-gradient force in an oceanic model with a nonaligned vertical coordinate. *Journal of Geophysical Research-Oceans*, **108,** art. no.-3090.

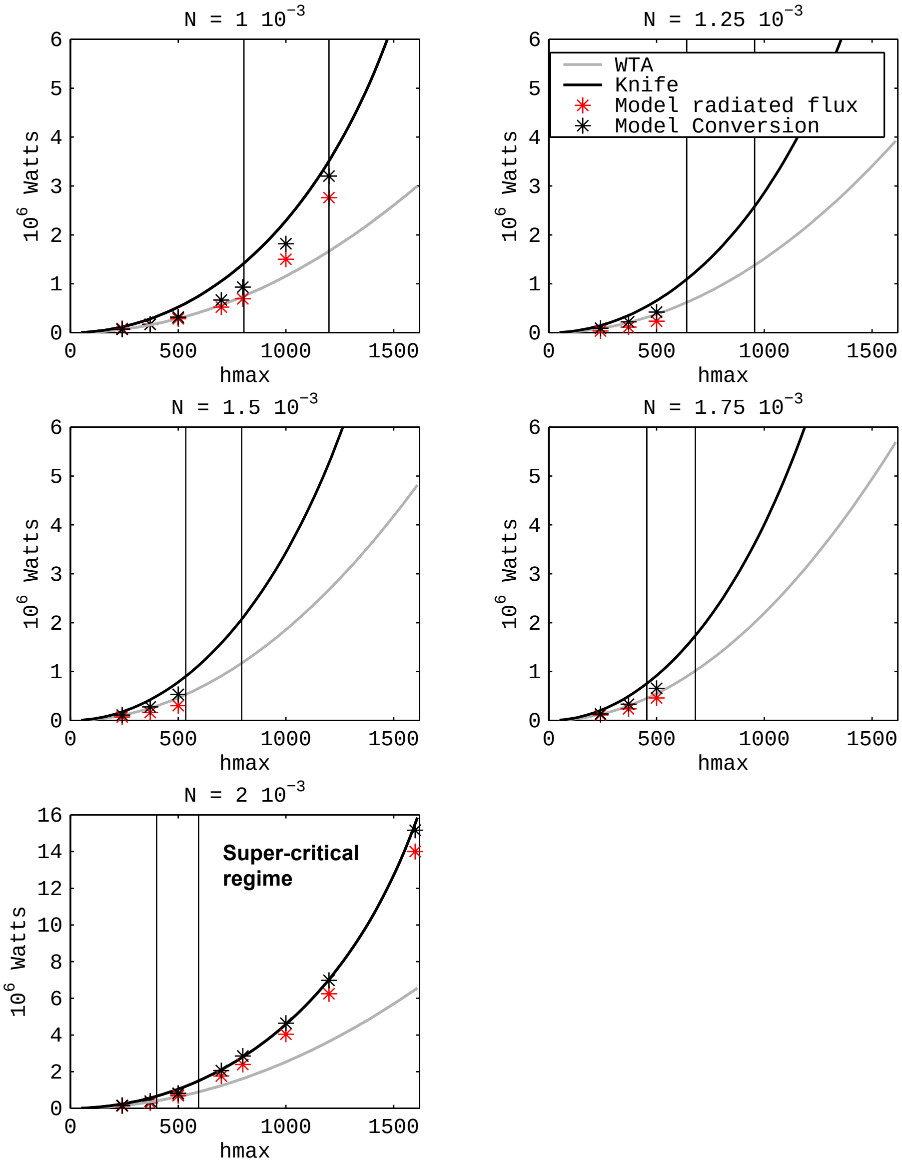

Figure 1 : Conversion diagrams from ROMS numerical model simulations (black stars). The wave energy flux radiated outward from the gaussian bump is also shown (red stars). Superimposed are the theory predictions for WTA and Knife (super-critical) regimes. Each panel represent the results obtained with different *N* (stratification) and h_{max} (height of the gaussian ridge in meters). In the model experiments the total depth of the ocean is 2000 m and the length of the model domain in the along ridge direction is 9000 m .The vertical black lines denote the model transition from sub-critical to super-critical (ε = [0.8 1.2]).

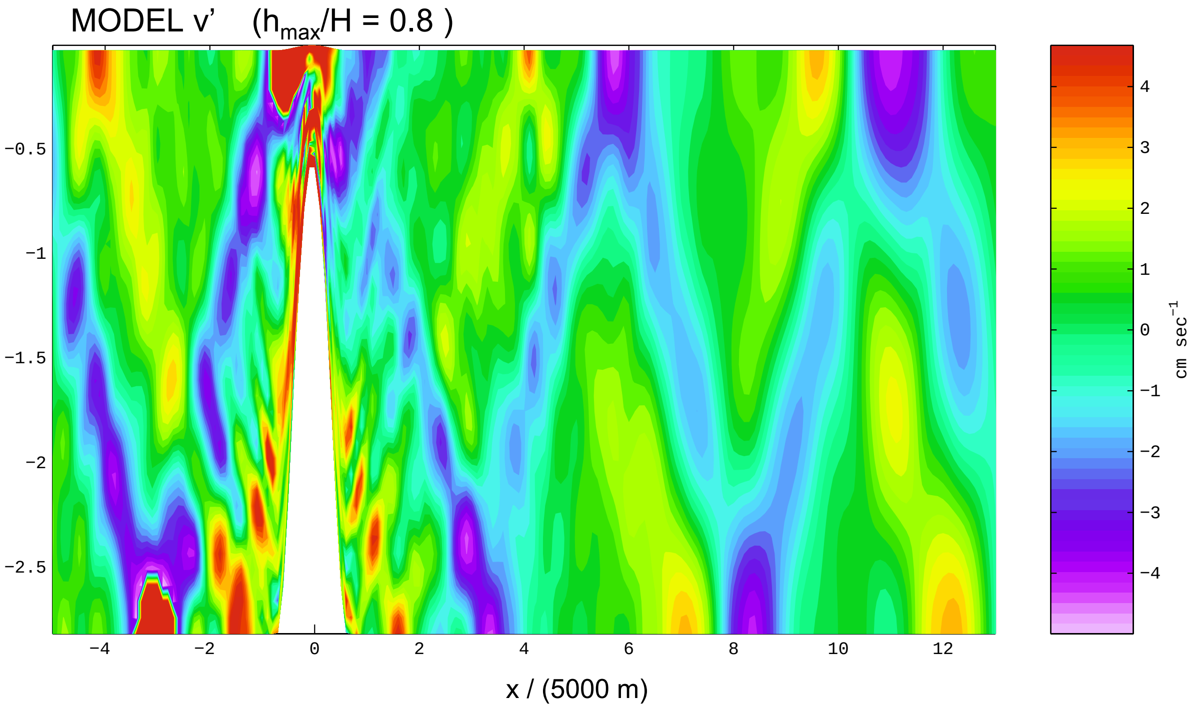

Figure 2: Velocity anomalies for the ROMS model case with ($h_{max}/H = 0.8$). The 0 on the x-axis indicates the location of the ridge.

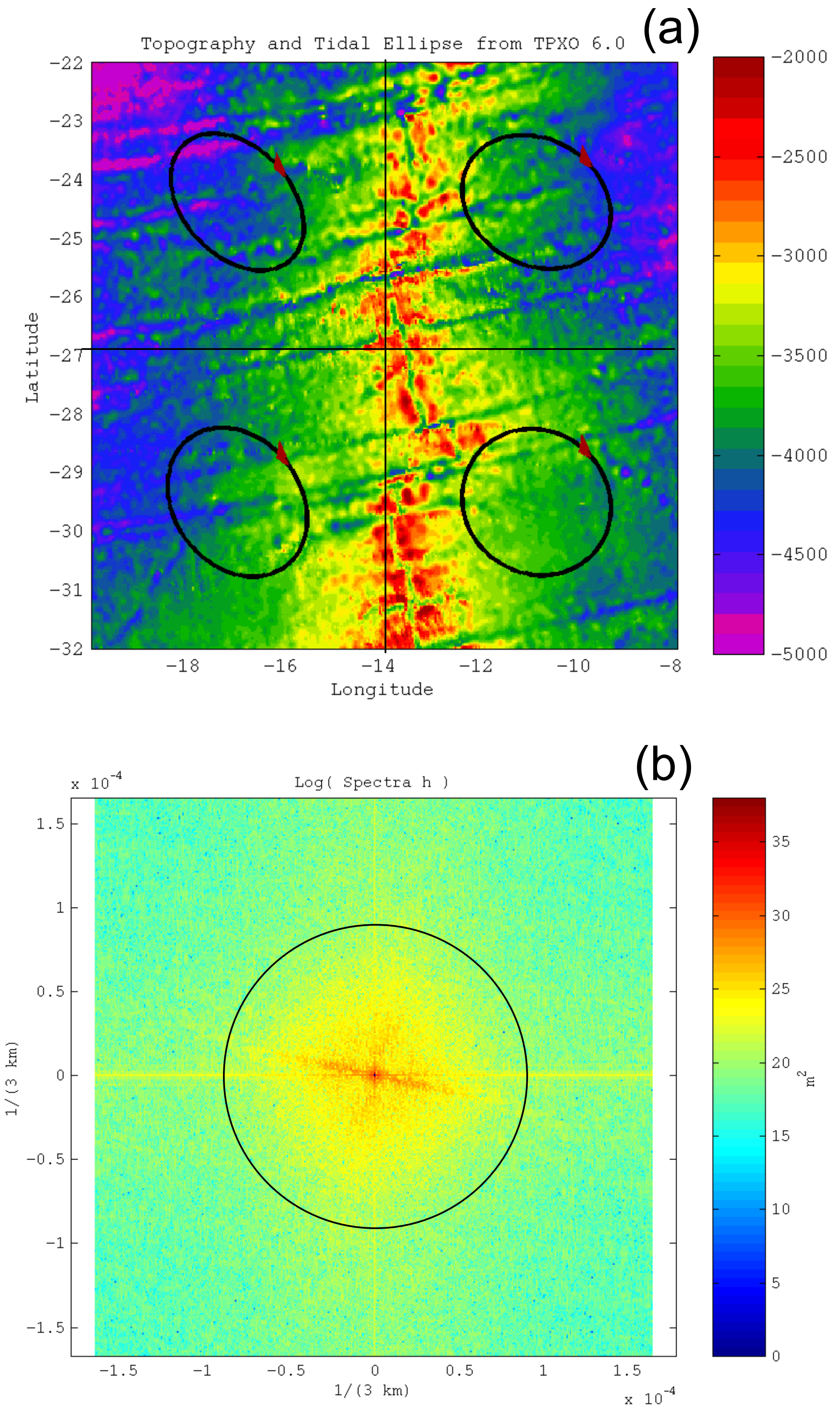

Figure 3: (a) Sandwell and Smith topography in a selected portion of the Atlantic Ocean. Overlapped the average tidal ellipse from the TPXO 6.0. The average is computed in each quadrant. (b) Spectra of the topography in (a) used to compute analytical conversion rates.